JOURNAL of the MEXICAN CHEMICAL SOCIETY
(J. Mex. Chem. Soc.)
Former Revista de la Sociedad Química de México (Rev. Soc. Quím. Méx.)

https://www.jmcs.org.mx/

Article

Open Access

J. Mex. Chem. Soc. **2026**, *70(1):e2438*

Received January 30th, 2025
Accepted April 15th, 2025

http://dx.doi.org/10.29356/jmcs.v70i1.2438
e-location ID: 2438

Keywords:
Polyethylene terephthalate (PET), polyethylene (PE), carbon sorbent, porous structure

Palabras clave:
Politereftalato de etileno (PET), polietileno (PE), sorbente de carbono, estructura porosa

***Corresponding author:**
Kalbaev Alisher
email: qalbaev.alisher.98@gmail.com

ISSN-e 2594-0317

A Study of the Structural Features and Textural Properties of Carbon Sorbents Derived from Recycled Polyethylene Terephthalate and Polyethylene Waste

Kalbaev Alisher[*,1], Abdikamalova Aziza[1], Asqarova Dilzoda[2], Khoshimov Shahrom[1], Paygamov Rahimjon[1], Bakhronov Khayot[3], Kholikov Kamoliddin[2], Salikhanova Dilnoza[1], Jumaeva Dilnoza[1], Eshmetov Izzat[1], Maratov Nursultan[1], Nozim Mamataliev[1]

[1]Institute of General and Inorganic Chemistry of the Academy of Sciences of the Republic of Uzbekistan, Tashkent, 77a, Mirzo Ulugbek str., 100170 Uzbekistan.
[2]Namangan Engineering-Technological Institute, Namangan, 7 Kosonsoy str., 160115 Uzbekistan.
[3]Tashkent University of Information Technologies named after Muhammad al-Khwarizmi, Tashkent, Amir Temur Avenue 108, 100084 Uzbekistan.

Abstract. This article presents the results of a study on carbon sorbents obtained from recycled polyethylene terephthalate (PET) and polyethylene (PE) waste. The research focused on analyzing the structural features and textural properties of the sorbents, as well as their adsorption capabilities. It was found that the specific surface area of sorbents derived from PET with the addition of oxidized graphite reached 318.76 m^2/g, while similar materials based on PE achieved up to 420.47 m^2/g. These parameters, combined with an increased volume of micropores and mesopores, significantly enhance adsorption efficiency, particularly in water purification applications.
The addition of a pore-forming resulted in a further increase in specific surface area, reaching 825.99 m^2/g for PET-OG10 and 1011.78 m^2/g for PE-OG10, making these materials particularly promising for adsorption processes. Experimental results confirmed that such carbon-based sorbents effectively remove heavy metals and organic pollutants from water due to their well-developed micro- and mesoporous structure. Thus, the findings of this study

highlight the potential of recycled polymeric materials for the development of novel high-performance sorbents, contributing to enhanced environmental safety and sustainable waste management.

Resumen. Este artículo presenta los resultados de un estudio sobre sorbentes de carbono obtenidos a partir de residuos reciclados de politereftalato de etileno (PET) y polietileno (PE). La investigación se centró en el análisis de las características estructurales y las propiedades texturales de los sorbentes, así como en su capacidad de adsorción. Se encontró que el área superficial específica de los sorbentes derivados del PET con la adición de grafito oxidado alcanzó los 318.76 m²/g, mientras que materiales similares basados en PE lograron hasta 420,47 m²/g. Estos parámetros, combinados con un aumento en el volumen de microporos y mesoporos, mejoran significativamente la eficiencia de adsorción, particularmente en aplicaciones de purificación de agua.

La adición de un porógeno resultó en un aumento adicional del área superficial específica, alcanzando 825.99 m²/g para PET-OG10 y 1011.78 m²/g para PE-OG10, lo que hace que estos materiales sean especialmente prometedores para los procesos de adsorción. Los resultados experimentales confirmaron que estos sorbentes a base de carbono eliminan eficazmente metales pesados y contaminantes orgánicos del agua, gracias a su estructura bien desarrollada de micro y mesoporos. Por lo tanto, los hallazgos de este estudio destacan el potencial de los materiales poliméricos reciclados para el desarrollo de nuevos sorbentes de alto rendimiento, contribuyendo así a una mayor seguridad ambiental y a una gestión sostenible de residuos.

Introduction

Global plastic production has reached approximately 8.3 billion tons since the advent of large-scale manufacturing in the 1950s, of which around 6.3 billion tons have turned into waste [1-3]. Of this waste, only 9 % has been recycled, 12% incinerated, and the remaining 79 % accumulated in landfills or the environment. These figures underscore the severity of the polymer waste disposal issue, driven by the extensive production and use of plastic materials. The primary sources of such waste include packaging materials, construction products, consumer goods, textiles, vehicles, and electrical equipment. In 2018 alone, the volume of plastic waste exceeded 343 million tons, with 90 % attributed to post-consumer waste [4].

The resistance of polymer waste to biodegradation exacerbates the problem of its accumulation in the environment. Traditional disposal methods, such as landfilling and incineration, have significant environmental drawbacks. Secondary recycling of plastics stands out as the most promising waste management approach; however, its effectiveness depends on the quality of waste collection and sorting, as well as advancements in recycling technologies [5–9].

The recycling of polymer waste is becoming increasingly important in the context of reducing environmental impact. Developed countries, such as the United States, Canada, Japan, Germany, the United Kingdom, and France, have successfully implemented recycling strategies, significantly reducing the volume of plastic waste. Meanwhile, in many developing countries, recycling rates remain low due to a lack of advanced infrastructure and technologies [10–12]. In this regard, the disposal of specific types of polymers, such as PET, warrants particular attention.

Polyethylene terephthalate (PET) is a polymer widely used in the production of plastic bottles due to its outstanding properties, such as strength, light weight, and chemical resistance [13]. Despite these advantages, the widespread use of PET bottles creates significant environmental challenges, particularly related to their disposal. Global consumption of PET bottles reached approximately 500 billion units in 2017, underscoring the urgent need for effective recycling measures [14]. Developing sustainable methods for the disposal and recycling of these materials is critically important to reducing environmental impact and promoting sustainable development.

The recycling of PET bottles involves mechanical recycling (collecting, sorting, washing, and shredding the bottles into pellets) and chemical recycling (depolymerizing PET into monomers for repolymerization). Incineration of heavily contaminated bottles is used for energy recovery but is associated with the release of harmful substances. The quality of secondary materials depends on the sorting of bottles by color and contamination levels.

Particular attention is given to the recycling of polyethylene caps made from high-density polyethylene, which are also used in the production of new products. Recently, numerous studies have emerged focusing on the development of sorbents from PET and PE waste, which can effectively treat wastewater while simultaneously addressing the issue of plastic waste disposal and contributing to environmental protection [15–18].

The aim of the research presented in this work is to develop and analyze effective methods for the disposal and recycling of PET and PE waste, with particular focus on the impact of adding oxidized graphite (OG) and a pore-forming on the structural properties of the resulting carbon materials. The study is aimed at enhancing the efficiency of plastic waste recycling into highly effective sorbents for wastewater treatment, which contributes not only to reducing the environmental impact of plastic waste but also to increasing its economic value.

Experimental

The primary materials selected for the study to produce carbon were polyethylene terephthalate (PET) and polyethylene (PE). These materials, derived from recycled waste, exhibit high chemical resistance and thermal stability, making them suitable for the production of carbon sorbents.

The main characteristics of such PET include:

Table 1. Key characteristics of PET bottles.

ρ, g/sm^3	**T_g, °C**	**T_m, °C**	**Tr, %**	**OP, mL/m²·**	**RI**	**S, m^2/g**	**MS, MPa**
1.335	37	265	90-91	0.04	1.57	0,5	62

Tr – Transparency; OP – Oxygen Permeability (O_2); RI – Refractive Index; MS – Mechanical Strength.

The experimental part of the study utilized polyethylene terephthalate (PET) bottles with key characteristics presented in Table 1. The density of PET is 1.335 g/cm³, which confirms its strength and resistance to mechanical stress. The glass transition temperature of the material is 37°C, indicating its ability to transition from a solid to an elastic state upon heating, while the melting temperature reaches 265°C, demonstrating its high thermal stability.

The transparency of PET bottles ranges from 90 % to 91 %, ensuring the possibility of visual inspection of the contents and making them suitable for beverage packaging. The oxygen permeability is 0.04 mL/m²·day·atm, which helps preserve the quality of packaged products by minimizing oxygen penetration. The refractive index reaches 1.57, reflecting the material's excellent optical properties. The mechanical strength of PET is 62 MPa, highlighting its high performance characteristics.

Table 2 presents the physicochemical properties of polyethylene (PE) caps.

Table 2. Physicochemical properties of polyethylene (PE) caps.

ρ, g/sm^3	**T_m, °C**	**OP, mL/m²·**	**MS, MPa**	**S, m^2/g**
0.99	110	0.05	51	0.4

The high-density polyethylene (HDPE) used in the experiment has a density of 0.99 g/sm³, indicating its high mechanical strength and resistance to stresses during sealing and transportation processes.

The melting temperature of HDPE is 110°C, reflecting its standard characteristics and ensuring the material's thermal stability at high temperatures without the risk of deformation.

The oxygen permeability of 0.05 mL/m²·day·atm indicates low gas permeability, contributing to the airtightness of the caps. The specific surface area of HDPE is 0.4 m²/g, highlighting the material's limited adsorption capacity. In this context, the low specific surface area is not a critical parameter, as the caps are not designed for adsorption functions.

Thermogravimetric studies were conducted using a Paulik-Paulik-Erdey system derivatograph. The samples were heated at a rate of 10 °C/min with a sample mass of 0.1 g. The derivatograph is equipped with a differential thermal analysis (DTA) cell and thermobalances for thermogravimetry, recording changes in mass and their rate. The DTA cell includes registrants for the temperature difference between the sample and the reference (aluminum oxide Al_2O_3), as well as the temperature of the sample itself.

To support the process and enhance the properties of the final product, the auxiliary materials «HYDROCEROL CF 40 E» pore-forming and oxidized graphite (GRAFT EG 350-50(80), with an expansion degree of 350 mL/g, oxidized with sulfuric acid) were used. The pore-forming is employed to create a foamed structure in polymer matrices, increasing the specific surface area and adsorption properties of the materials. Oxidized graphite is added as a functional filler, improving the mechanical, thermal, and adsorption characteristics of the final composites.

The mixing of the components was carried out in the following sequence: pre-crushed PET and PE waste (particle size 1–3 mm) was weighed according to the specified formulation. Calculated amounts of oxidized graphite (within the range of 1–10 wt.%) and blowing agent (0.5–2 wt.%) were subsequently added to the polymer mass. The mixture was thoroughly blended in dry form using a ball mill at room temperature for 20–30 minutes until a homogeneous composition was obtained. If necessary, additional manual homogenization was performed to prevent filler agglomeration.

The prepared mixture was loaded into a thermal treatment reactor. The thermal processing was carried out for 2 hours at a temperature of 700–1000 °C in an argon atmosphere. This approach prevented oxidative processes and ensured complete carbonization of the polymer matrix, resulting in the formation of a porous carbon structure.

The thermal treatment of the samples was carried out in a laboratory setup for pyrolysis and thermoactivation at the "Colloid Chemistry and Industrial Ecology" laboratory of the Institute of General and Inorganic chemistry of Academy of Sciences of the Republic of Uzbekistan [19]. The setup includes a sealed reactor with an electric heater, ensuring uniform heating of the raw material to the desired temperature. The reactor operates in an inert gas atmosphere (argon) to prevent oxidation. The raw material is placed on a stainless-steel reaction mesh inside the reactor. The process temperature is monitored by a thermocouple connected to the unit to maintain stable conditions. The gases released are diverted and analyzed, allowing for precise control of the gas composition and optimization of the carbon adsorbent production process.

The surface morphology was analyzed using scanning electron microscopy (SEM), while the elemental composition of the carbons was studied using energy-dispersive spectroscopy (EDS) (Jeol model JSM-21).

To determine the characteristics of the porous structure, such as specific surface area (S), total pore volume (ΣV), and pore diameter (d_{pore}), the method of low-temperature nitrogen adsorption at 77 K was used on a Quantachrome Nova 1000e apparatus. The samples were pretreated in a vacuum at 100°C for 12 hours. The partial pressure reached 0.995 P/P_0. Adsorption and desorption isotherms of nitrogen were measured over a range of partial pressures from 0.005 to 0.995 P/P_0 and processed using the BET method. The micropore volume was determined by the t-Plot method, while the mesopore volume was calculated using the BJH method. The average pore diameter was estimated using the formula $D_{avg} = 4V/S$. The micropore size distribution, with an average size of 1.15–1.17 nm, was assessed using the Horvath-Kawazoe (HK) method.

Results and discussion

Thermogravimetric analysis (TGA) is crucial for the study of carbon adsorbents, as it provides important data on the thermal behavior and stability of materials. This information is critical for determining the optimal conditions for pyrolysis and activation, which directly influence the quality and efficiency of carbon adsorbents.

TGA allows for the identification of decomposition temperature ranges and stable phases of materials, which is essential for the development of technologies for their application in environmental remediation.

The obtained results of the thermal analysis are presented in Fig. 1.

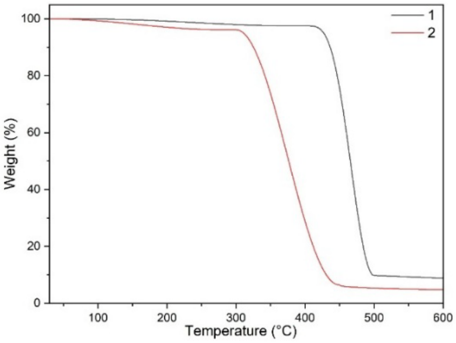

Fig. 1. Thermogram of the samples **(1)** PET, **(2)** PE.

The thermogram displays the thermal decomposition processes of PET and PE. PET exhibits thermal stability, maintaining its mass up to approximately 400 °C due to its polycrystalline structure and strong ester bonds [20]. The main decomposition of PET occurs between 420–500 °C, accompanied by a sharp mass loss due to the breakdown of ester bonds [21]. In contrast to PET, the thermal decomposition of PE begins at approximately 300 °C, which is attributed to its amorphous structure and the breakdown of carbon–carbon bonds, accompanied by the formation of volatile organic compounds. [22]. For PE, decomposition proceeds up to 450 °C. Both materials stabilize after 500 °C, indicating the completion of the thermal decomposition process.

Subsequently, the samples of PET and PE were carbonized to obtain carbons.

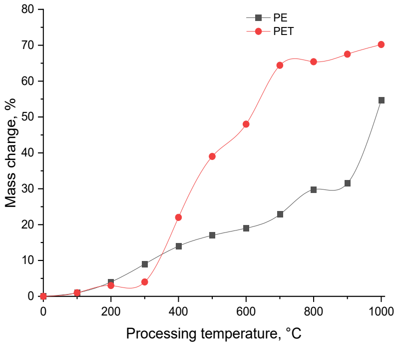

Fig. 2. Mass change during the thermal treatment of polymers over a 2-hour period.

The graph depicts the mass variation of PE and PET as a function of temperature in an inert atmosphere. Below 300 °C, mass losses for both polymers are minimal, which is associated with the removal of residual moisture and volatile low-molecular-weight compounds. In the temperature range of 300–500 °C, polyethylene undergoes active decomposition, driven by the gradual breakdown of carbon–carbon bonds, resulting in an increasing rate of mass loss.

For PET, a significant mass loss begins at around 400 °C and reaches its maximum in the range of 500–700 °C. This is attributed to the intensive breakdown of the polyester chain and the release of volatile products of thermal degradation.

After 700 °C, the rate of mass loss decreases for both polymers, indicating the completion of the main stage of thermal decomposition. At 1000 °C, the residual mass of PE is approximately 45.3 %, while for PET, it is 29.8 %, which is significantly lower than the theoretical carbon content, indicating the intensive release of volatile products and limited formation of carbon residue.

Thermal treatment of polymer materials, such as PE and PET, involves processes of thermal degradation and the formation of carbon residues [23-26]. The addition of a filler, such as oxidized graphite (OG), before thermal treatment can significantly influence these processes [27]. Due to its thermochemical stability, developed porous structure, and catalytic properties, OG contributes to altering the degradation kinetics of the polymers, increasing the yield of the carbon residue, and optimizing the structure of the resulting carbon.

The study of the influence of oxidized graphite (OG) on the thermal behavior of PET and PE is crucial for the development of carbon adsorbents with specific characteristics. OG can act as a catalyst, accelerating thermal transformations and promoting the formation of a porous structure in the carbon material. This also affects the degree of crystallinity of the carbon. The joint treatment of polymers and OG allows for the investigation of interactions between the components and the identification of conditions that lead to the formation of carbon materials with optimized properties.

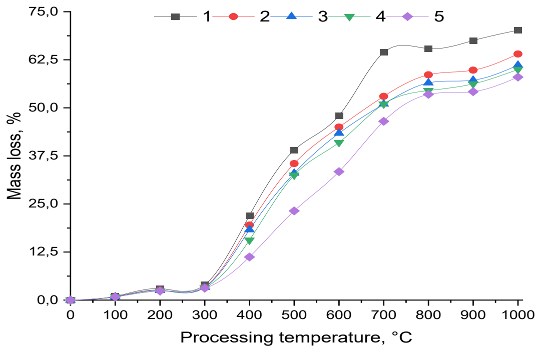

Fig. 3. Mass change during thermal treatment (2 hours) of the PET-OG mixture at different OG contents (%).

To investigate the effect of oxidized graphite (OG) on the mass change and structure of carbon materials, PET-OG and PE-OG mixtures were prepared with OG mass content ranging from 1 to 10% (fig. 3-4). Systems with higher OG content were not studied, considering economic feasibility and rational resource utilization.

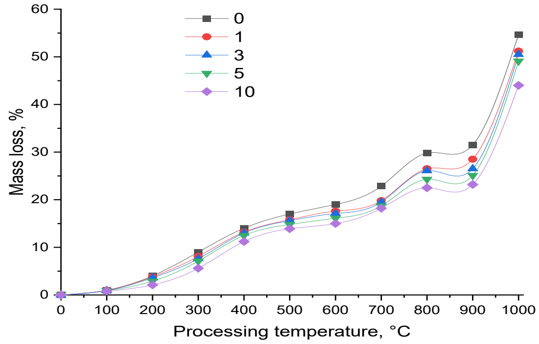

Fig. 4. Mass change during thermal treatment (2 hours) of the PE-OG mixture at different OG contents (%).

The data presented in Fig. 3 show that in the temperature range up to 300 °C, mass losses are minimal and do not exceed 4 % for all samples, regardless of the OG content. This indicates a negligible thermal effect in this region, primarily caused by the removal of moisture and unstable low-molecular-weight compounds.

The thermal effect in this region is primarily due to the removal of moisture and unstable low-molecular-weight compounds. Starting from 400°C, a sharp increase in mass loss is observed, corresponding to the main stage of thermal degradation of PET, associated with the breakdown of the polymer chain. The stabilizing effect of OG is clearly evident: at 400°C, the mass loss of pure PET is 22 %, while for the composition with 10 % OG, it is only 11.2 %. As the temperature increases, this effect becomes more pronounced: at 500 °C, the mass loss reaches 39 % for unmodified PET, while it is only 23.2 % for the composition with 10 % OG.

In the temperature range of 600–800 °C, destruction and gasification continue, but the rate of mass loss decreases. A clear trend is also observed in this range: the higher the OG content, the lower the total mass loss. For example, at 700 °C, the mass loss decreases from 64.4 % (0% OG) to 46.5 % (1 0% OG), and at 800 °C, it decreases from 65.4 % to 53.5 %.

In the final stage (900–1000 °C), mass loss continues, but it is less pronounced. OG still demonstrates a protective effect: at 1000 °C, the residual mass is 41.7 % for pure PET (mass loss of 70.2 %), while with the addition of 10 % OG, the residual mass is higher — around 42 % (mass loss of 58 %).

In contrast to PET, the thermal decomposition of PE occurs more smoothly, without a pronounced abrupt transition in the range of 400–700 °C (Fig. 4). The differences between samples with varying OG content are mainly observed in the final stages of pyrolysis (above 800°C), while in PET, the effect of OG is noticeable starting from 400 °C.

For PE, the addition of oxidized graphite reduces the total mass loss to a lesser extent: at 1000 °C, the difference between pure PE and the sample with 10 % OG is about 10.7 %, while for PET, it is more than 12 %. Moreover, PE retains a higher residual mass at the same temperatures, indicating a more thermally stable hydrocarbon residue compared to PET.

Thus, OG has a more pronounced stabilizing effect on the thermal degradation of PET than on PE, especially during the mid-temperature stage (400–700 °C).

OG also promotes the formation of a porous structure in the carbon, acting as a template for pore development. This contributes to the enhancement of the micro- and mesoporous structure of the carbon during pyrolysis, as evidenced by the reduced mass at higher OG contents, indicating complex changes in the PET degradation process and improvements in the porous characteristics of the carbon structure.

Thus, the addition of oxidized graphite influences the thermal processes of carbonization and the quality of the final carbon adsorbents, allowing for the optimization and control of the properties of the resulting materials.

To understand the mechanisms of the structure of carbon adsorbents made from PE and PET with the addition of oxidized graphite (OG), a detailed analysis of morphology and composition was conducted. The interaction of OG with the polymers during thermal treatment significantly affects the porosity and adsorption properties of the adsorbents, altering the polymer decomposition and the structure of the carbon matrix. This leads to modifications in the morphology and an increase in carbon content.

The following presents the results of studies on carbon materials derived from PE-OG and PET-OG, demonstrating the influence of OG on the structure of the adsorbents. The microscopic images in Fig. 5 show the differences in the structure of the carbon materials from PE and PET, thermally treated at 700 °C. The carbon from PE exhibits a compact and dense structure with minimal porosity, showing smooth areas and isolated inclusions, indicating low structural heterogeneity.

The carbon derived from PET in the same image contains both dense areas and rounded pores with fine textural differences, reflecting partial pore formation. This pore formation is caused by the presence of ester groups in PET, which promote gas formation and the creation of micropores during thermal decomposition.

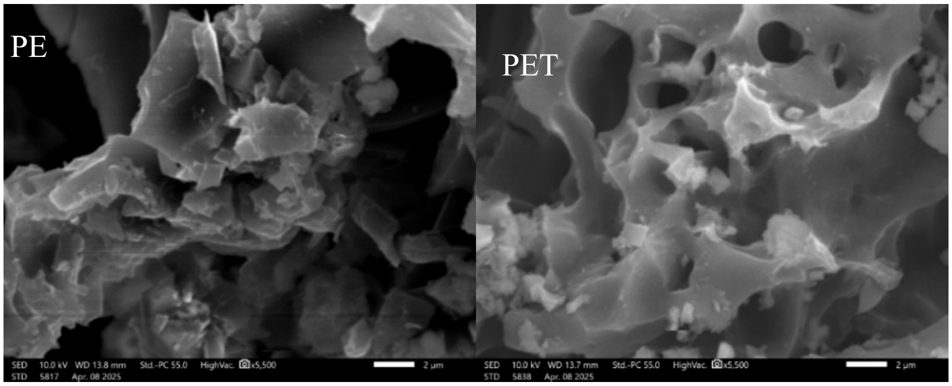

Fig. 5. Microscopic images of the carbons obtained at a temperature of 700 °C.

ISSN-e 2594-0317

During thermal treatment at 700 °C, both materials exhibit low porosity, likely due to the absence of conditions required for pore development, such as activation. However, the carbon derived from PET demonstrates more pronounced structural heterogeneity.

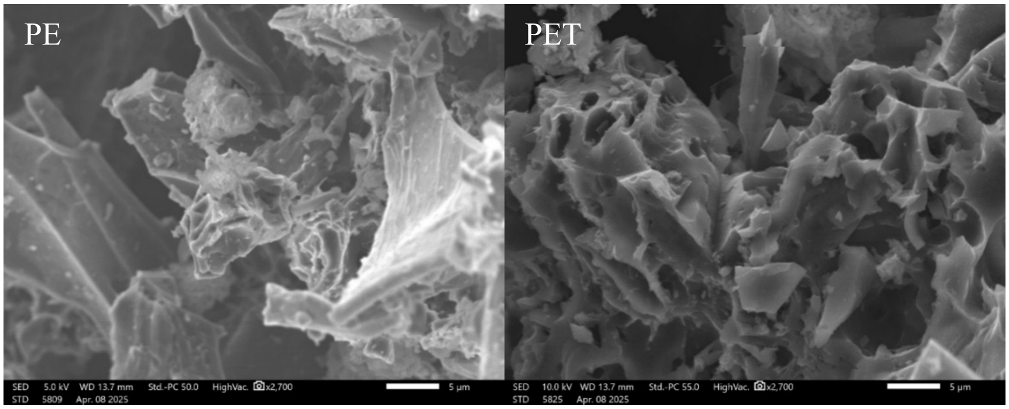

Fig. 6. Microscopic images of the carbons obtained at a temperature of 700°C with the addition of 1 % OG.

Microscopic images of the carbons derived from PE and PET with the addition of 1 % oxidized graphite (OG) and thermal treatment at 700 °C show noticeable structural changes. The PET carbon with OG exhibits increased porosity with rounded pores, indicating the role of OG as a "template" for pore formation, enhanced by gas release during PET degradation and the catalytic effect of OG.

In the PE carbon with OG, localized surface degradation is observed, indicating a less porous structure, although the presence of OG contributes to an increase in surface heterogeneity and an improvement in adsorption properties. The addition of OG has a more noticeable impact on the structure of the PET carbon due to its complex ester structure, which facilitates the formation of a well-developed porosity.

Increasing the OG content to 10% enhances the surface heterogeneity through the agglomeration of OG particles, creating localized areas with varying porosity. This amplification of the structural heterogeneity of the carbons occurs due to the catalytic influence of OG and intense gas release when OG interacts with the polymer degradation products, leading to the formation of carbons with varying densities.

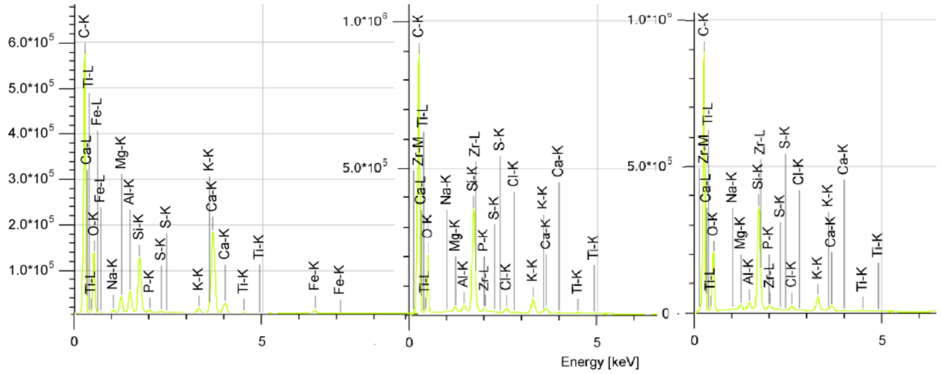

Fig. 7. Elemental composition of PET at different OG contents (%): 1) 0; 2) 1; 3) 3.

As the content of oxidized graphite (OG) increases to 10% in the carbon materials obtained through thermal treatment, an increase in the intensity of the carbon signal is observed in the energy-dispersive X-ray spectroscopy (EDS) spectra. This indicates a higher proportion of the carbon phase in the sample composition. This is due to the

J. Mex. Chem. Soc. **2026**, *70(1):e2438*
Regular Issue

ISSN-e 2594-0317

incorporation of additional carbon from OG into the structure of the carbon materials. At 3% OG content, the intensity of the carbon signal significantly increases, confirming the accumulation of the carbon phase.

With the increase in carbon content, a decrease in the relative signals of oxygen and other elements is observed due to the decomposition of oxygen-containing groups in OG at high temperatures. This indicates the carbonization of materials and the transformation of oxygen-containing structures into carbon ones. The presence of elements such as silicon (Si), aluminum (Al), calcium (Ca), and titanium (Ti) is attributed to the composition of the starting materials and mineral impurities in the OG.

Elemental composition analysis shows that increasing the content of oxidized graphite (OG) in PET-based char increases the carbon content from 68.2 % to 72.5 % and reduces the oxygen content from 28.8 % to 26.1 %. Similar changes were observed in PE-based char, where the carbon content increased from 72.2 % to 79.8 %, and the oxygen content decreased from 23.6 % to 18.3 %.

These data confirm the significant impact of oxidized graphite (OG) on the structural and chemical properties of char obtained from PE and PET, where the increase in OG content promotes carbonization, improves the porous structure, and, consequently, enhances the adsorption properties. The presence of mineral impurities from OG and polymers does not significantly affect the carbonization process, highlighting the effectiveness of OG in improving the quality of carbon adsorbents.

Pore-formings are critically important for creating the porous structure of carbon materials, influencing their adsorption characteristics [28,29]. The use of pore-formingic agents, such as Hydrocerol CF 40 S, allows for the control of pore size and distribution, increasing the specific surface area of the char. This pore-forming, by absorbing heat during decomposition and releasing CO_2, contributes to the formation of uniform porosity without releasing nitrogen, minimizing the chemical impact on the material.

Fig. 8 presents micrographs of carbon materials derived from PE and PET with 10 % oxidized graphite (OG) and varying amounts of pore-forming, illustrating changes in morphology that are critical for adsorption processes.

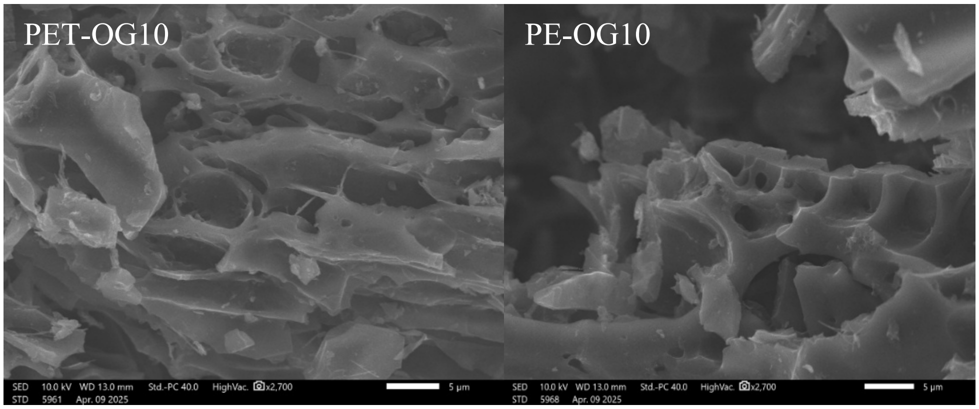

Fig. 8. Micrographs of the carbon samples obtained with 0.5 % pore-forming content.

The comparison of carbons from PET-OG10 and PE-OG10 mixtures with the addition of 0.5 % pore-forming reveals noticeable differences in morphology compared to the samples without the pore-forming. The microscopic images of these carbons demonstrate a well-developed texture and clearly expressed porosity, highlighting the significant impact of the pore-forming on structural formation. Both types of carbons with pore-forming exhibit increased heterogeneity, with the presence of small pores and microcracks formed as a result of the thermal degradation of the mixture. This indicates that the blowing agent promotes porosity and increases the specific surface area through the release of gases during thermal treatment.

Carbons without the pore-forming have a more compact structure with limited porosity, indicating a significant restriction in pore formation in the absence of the pore-forming, which facilitates the rupture of the polymer matrix during pyrolysis.

ISSN-e 2594-0317

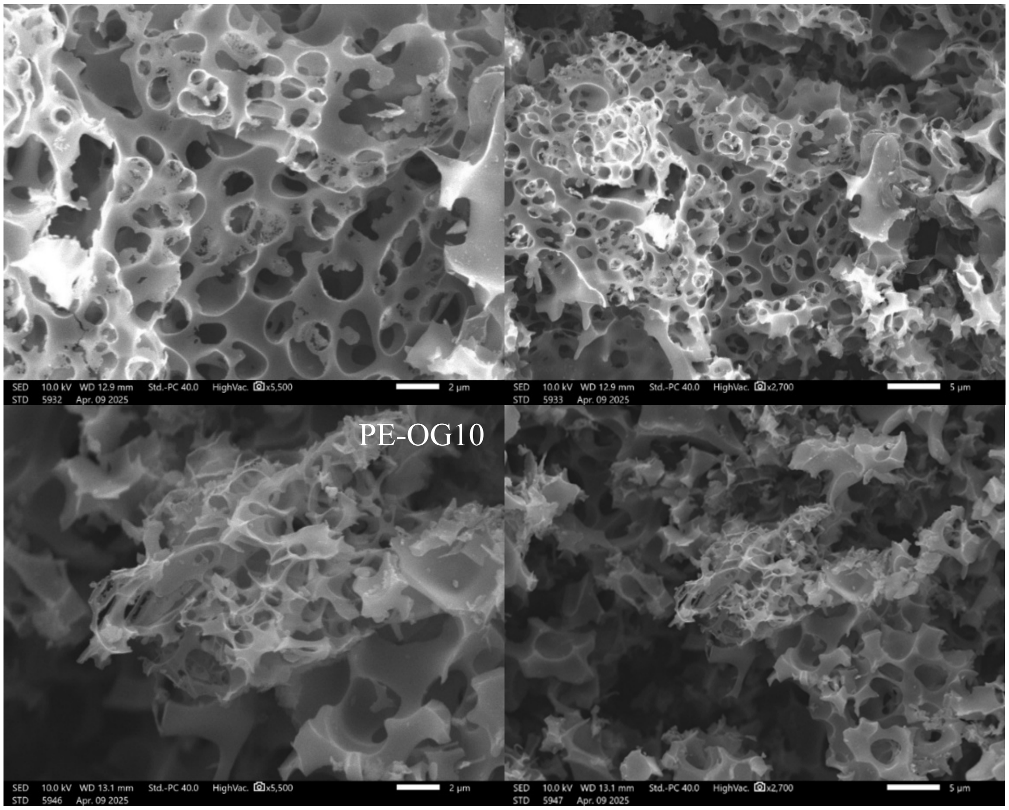

Fig. 9. Microscopic images of carbons (magnification 900× and 1500×) obtained with the addition of 2% pore-forming.

Microscopic images of PET-OG10 (samples 1 and 2) and PE-OG10 (samples 3 and 4) carbons with the addition of 2 % pore-forming show a significant increase in porosity compared to the corresponding carbons without the pore-forming. The PET-OG10 samples demonstrate finer pores and a more uniform distribution of particles, thanks to the polycrystalline structure of PET, which promotes the formation of a finely dispersed carbon matrix. In contrast, the carbons based on PE-OG10 have larger pores and a less uniform distribution, reflecting the amorphous structure of PE, which facilitates the formation of larger aggregates during thermal treatment.

The addition of 2 % pore-forming leads to a significant improvement in overall porosity and specific surface area in both types of carbons. The carbons derived from PET show a finer and more uniform structure, potentially providing better sorption properties for applications requiring high specific surface area.

Thus, the use of the pore-forming Hydrocerol CF 40 S with polymeric waste materials such as PET and PE enables the production of carbon adsorbents with improved textural characteristics. The formed porous structure significantly enhances the sorptive capacity of the carbons, making them effective for water and air purification.

The next section of the article presents nitrogen adsorption isotherms, which are a key tool for analyzing the porous structure of carbon adsorbents. The results of the nitrogen adsorption isotherms provide valuable information about the ability of the carbons to adsorb contaminants, forming the basis for their application in purification systems [30,31].

J. Mex. Chem. Soc. **2026**, *70(1):e2438*
Regular Issue

ISSN-e 2594-0317

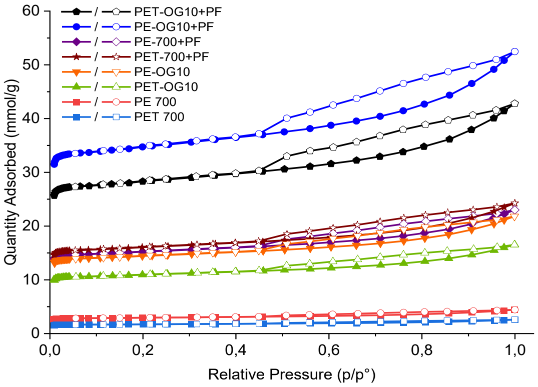

Fig. 10. Nitrogen adsorption-desorption isotherms for carbon samples.

The nitrogen adsorption-desorption isotherms for the carbon samples indicate a mesoporous structure, corresponding to type IV with hysteresis typical of slit-shaped pores. The PET-700 and PE-700 samples exhibit flatter isotherms, suggesting a less developed porous structure, in contrast to PET-OG10 and PE-OG10, where a higher amount of nitrogen is adsorbed due to the more developed porosity promoted by the addition of oxidized graphite (OG).

The hysteresis loops of the PET-OG10 and PE-OG10 samples show an H3 type, indicating the presence of slit-shaped mesopores. These data emphasize the improved pore structure resulting from the use of OG.

The addition of a pore-forming agent leads to a significant increase in the specific surface area and pore volume, particularly noticeable in the relative pressure range of 0.4-0.8, highlighting its role in the development of the textural characteristics of carbon materials and improving their adsorption properties.

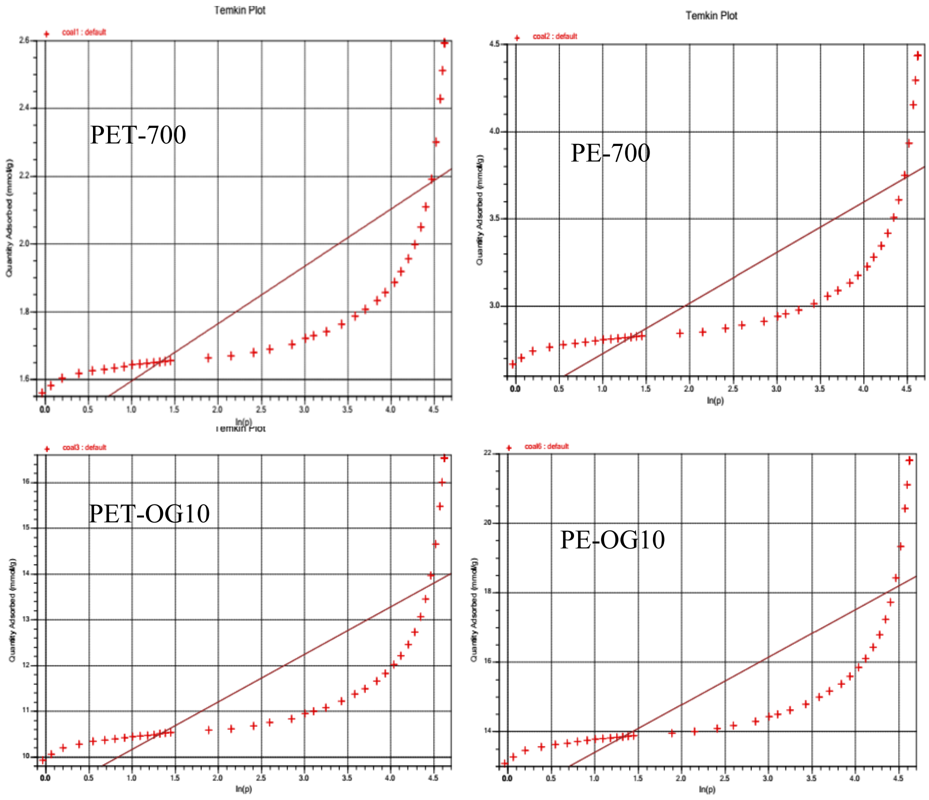

http://dx.doi.org/10.29356/jmcs.v70i1.2438

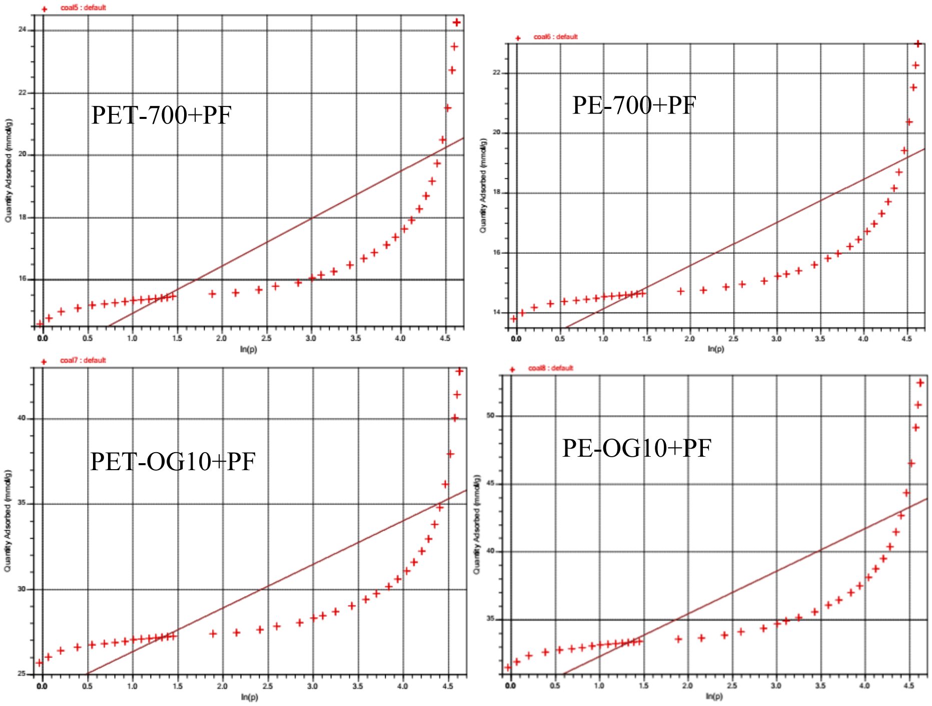

Fig. 11. Temkin plot for the investigated samples.

The Temkin plots for nitrogen adsorption analysis on the PET-700, PE-700, and graphite oxide-modified samples PET-OG10 and PE-OG10 reveal significant differences in adsorption properties. The linear portions of the plots indicate that the adsorption follows the Temkin model, reflecting physical adsorption with moderate interaction energy [32,33]. This suggests the heterogeneity of the adsorbent surfaces with varying energies of active centers.

The PET-700 and PE-700 samples exhibit low values of adsorbed nitrogen, indicating low porosity and a limited volume of micropores. In contrast, the PE-OG10 carbons demonstrate significantly higher adsorption capacity due to an increased number and size of pores created during degradation with the addition of 10 % graphite oxide. This contributes to the formation of a mesoporous structure, which enhances nitrogen molecule retention.

The addition of a pore-forming agent to the carbon materials also leads to a significant increase in adsorption capacity, particularly at high pressures. The plots for the samples with pore-forming agents show elevated adsorption values, highlighting the increase in overall porosity and specific surface area, which positively affects the adsorption properties.

Table 3. Textural characteristics of the samples.

Sample	**S, m^3/g**	**t-Plot, m^3/g (surface of micropores)**	**V$_a$, sm^3/g**	**V$_b$, sm^3/g**
PET-700	50.04	27.79	0.050	0.038
PE-700	85.59	47.53	0.085	0.065
PET-OG10	318.76	176.66	0.317	0.244

J. Mex. Chem. Soc. **2026**, 70(1):e2438
Regular Issue
©2026, Sociedad Química de México
ISSN-e 2594-0317

Sample	**S, m^3/g**	**t-Plot, m^3/g (surface of micropores)**	**V$_a$, sm^3/g**	**V$_b$, sm^3/g**
PE-OG10	420.47	233.02	0.418	0.321
PET-700+PF	469.92	259.92	0.466	0.358
PE-700+PF	420.47	233.03	0.418	0.321
PET-OG10+PF	825.99	457.01	0.820	0.631
PE-OG10+PF	1011.78	560.78	1.006	0.774

The carbon materials PET-700 and PE-700 show differences in specific surface area, with PE-700 having 85.59 m^2/g and PET-700 showing 50.04 m^2/g, reflecting the impact of polyethylene thermal degradation on the formation of porous structure. When oxidized graphite (OG) is added, the specific surface area increases to 318.76 m^2/g for PET-OG10 and 420.47 m^2/g for PE-OG10.

The addition of a pore-forming further enhances the specific surface area, with maximum values achieved for PET-OG10+PF (825.99 m^2/g) and PE-OG10+PF (1011.78 m^2/g), demonstrating the synergistic effect of OG and pore-forming. Samples containing only pore-forming also show an increase in specific surface area, but to a lesser extent compared to the combination of OG and pore-forming.

The micropore volume also increases with the addition of OG and pore-forming, reaching the highest values for PE-OG10+PF (1.006 sm^3/g) and PET-OG10+PF (0.820 sm^3/g), which confirms the effectiveness of these additives in developing the porous structure. These data indicate improved textural characteristics of the carbons, making them suitable for use in adsorption technologies.

Conclusions

The results of the study on the thermal processing of polyethylene terephthalate (PET) and polyethylene (PE) waste, as well as the impact of adding oxidized graphite (OG) and pore-forming on the porous structure and adsorption properties of the resulting carbon materials, were discussed. It was found that the specific surface area of the PET-700 carbon material was 50.04 m^2/g, and that of PE-700 was 85.59 m^2/g. After the addition of OG, these values increased significantly: for PET-OG10, the specific surface area reached 318.76 m^2/g, and for PE-OG10, it reached 420.47 m^2/g. With the further addition of pore-forming, the specific surface area for PET-OG10+PF increased to 825.99 m^2/g, and for PE-OG10+PF, it reached 1011.78 m^2/g, confirming the synergistic effect of these additives.

The nitrogen adsorption isotherms showed that the presence of OG and pore-forming significantly improves the adsorption characteristics of the materials, increasing the volume of micropores and mesopores. Specifically, the maximum micropore volume was achieved for PE-OG10+PF (1.006 sm^3/g) and PET-OG10+PF (0.820 sm^3/g), while the maximum mesopore volume for these samples was 0.774 sm^3/g and 0.631 sm^3/g, respectively.

Thus, this study demonstrates that using PET and PE waste as starting materials for producing carbon adsorbents, modified with OG and pore-forming, offers a significant enhancement of their structural and functional properties. This opens up prospects for their application in various fields, including environmentally significant purification technologies.

J. Mex. Chem. Soc. **2026**, *70(1):e2438*
Regular Issue
©2026, Sociedad Química de México
ISSN-e 2594-0317

References

1. Rhodes, C.J. *Sci. Prog.* **2018**, *101*, 207–260. DOI: https://doi.org/10.3184/003685018X15294876706211
2. Hammer, J.; Kraak, M.H.; Parsons, J.R. *Rev. Environ. Contam. Toxicol.* **2012**, *220*, 1–44. DOI: https://doi.org/10.1007/978-1-4614-3414-6_1
3. Landrigan, P.J.; Raps, H.; Cropper, M.; Bald, C.; Brunner, M.; Canonizado, E.M.; … Dunlop, S. *Ann. Glob. Health* **2023**, *89*, 23. DOI: https://doi.org/10.5334/aogh.4331
4. Williams, A.T.; Rangel-Buitrago, N. *Mar. Pollut. Bull.* **2022**, *176*, 113429. DOI: https://doi.org/10.1016/j.marpolbul.2022.113429
5. Afshar, S.V.; Boldrin, A.; Astrup, T.F.; Daugaard, A.E.; Hartmann, N.B. *J. Clean. Prod.* **2024**, *434*, 140000.
6. Dey, S.; Veerendra, G.T.N.; Anjaneya Babu, P.S.S.; Phani Manoj, A.V.; Nagarjuna, K. *Biomater. Devices*. DOI: https://doi.org/10.1007/s44174-023-00085-w
7. Alaghemandi, M. *Sustainability.* **2024**, *16*, 10401. DOI: https://doi.org/10.3390/su162310401
8. Kumar, R.; Verma, A.; Shome, A.; Sinha, R.; Sinha, S.; Jha, P.K.; Kumar, R.; Kumar, P.; Shubham; Das, S.; et al. *Sustainability* **2021**, *13*, 9963. DOI: https://doi.org/10.3390/su13179963
9. Cubas, A.L.V.; Moecke, E.H.S.; Provin, A.P.; Dutra, A.R.A.; Machado, M.M.; Gouveia, I.C. *Polymers (Basel).* **2023**, *15*, 3151. DOI: https://doi.org/10.3390/polym15153151
10. Tumu, K.; Vorst, K.; Curtzwiler, G. *J. Environ. Manage.* **2023**, *348*, 119242. DOI: https://doi.org/10.1016/j.jenvman.2023.119242
11. Tsuchimoto, I.; Kajikawa, Y. *Sustainability.* **2022**, *14*, 16340. DOI: https://doi.org/10.3390/su142416340
12. Dokl, M.; Copot, A.; Krajnc, D.; Fan, Y.V.; Vujanović, A.; Aviso, K.B.; Tan, R.R.; Kravanja, Z.; Čuček, L. *Sustainable Production and Consumption.* **2024**, *51*, 498–518. DOI: https://doi.org/10.1016/j.spc.2024.09.025
13. Joseph, T.M.; Azat, S.; Ahmadi, Z.; Jazani, O.M.; Esmaeili, A.; Kianfar, E.; Haponiuk, J.; Thomas, S. *Case Stud. Chem. Environ. Eng.* **2024**, *9*, 100673. DOI: https://doi.org/10.1016/j.cscee.2024.100673
14. Massoud, T.; Dsilva, J. *Next Sustainability.* **2025**, *6*, 100095. DOI: https://doi.org/10.1016/j.nxsust.2024.100095
15. Dayal, L.; Yadav, K.; Dey, U.; Das, K.; Kumari, P.; Raj, D.; Mandal, R.R. *J. Hazard. Mater. Adv.* **2024**, *16*, 100460. DOI: https://doi.org/10.1016/j.hazadv.2024.100460
16. Mendoza-Carrasco, R.; Cuerda-Correa, E.M.; Alexandre-Franco, M.F.; Fernández-González, C.; Gómez-Serrano, V. *J. Environ. Manage.* **2016**, *181*, 522–535. DOI: https://doi.org/10.1016/j.jenvman.2016.06.070
17. Almazán-Almazán, M.C.; Pérez-Mendoza, M.; Domingo-García, M.; Fernández-Morales, I.; López, F.J.; López-Garzón, F.J. *Fuel Process. Technol.* **2010**, *91*, 236–242. DOI: https://doi.org/10.1016/j.fuproc.2009.10.003
18. Rai, P.; Singh, K. P. *J. Environ. Manage.* **2018**, *207*, 249–261. DOI: https://doi.org/10.1016/j.jenvman.2017.11.047
19. Khoshimov, S.; Raxmonaliyeva, N.; Askarova, D.; Seytnazarova, O.; Abdikamalova, A. *AIP Conf. Proc.* **2024**, *3045*, 030059. DOI: https://doi.org/10.1063/5.0197789
20. Alhulaybi, Z.; Dubdub, I. *Polymers*, **2023**, *15*. DOI: https://doi.org/10.3390/polym15143010
21. Turnbull, L., Liggat, J. J., & Macdonald, W. A. *Polym. Degrad. Stab.* **2013**, *98*, 2244–2258. DOI: https://doi.org/10.1016/j.polymdegradstab.2013.08.018
22. EP0273274B1. Degradation of polyethylene by means of agents generating free radicals. Applicant: Elf Atochem Deutschland GmbH (DE). Publication date: 12 July 2000. Bulletin 2000/28. Application No. 87118394.3, filed 11 Dec 1987, priority date: 11 Dec 1986 (DE3642266). Available at: https://patents.google.com/patent/EP0273274B1/en

23. Chia, J.W.F.; Sawai, O.; Nunoura, T. *Waste Manag.* **2020**, *108*, 62–69. DOI: https://doi.org/10.1016/j.wasman.2020.04.035
24. Chen, S.; Liu, Z.; Jiang, S.; Hou, H. *Sci. Total Environ.* **2020**, *710*, 136250. DOI: https://doi.org/10.1016/j.scitotenv.2019.136250
25. Dimitrov, N.; Kratofil Krehula, L.; Ptiček Siročić, A.; Hrnjak-Murgić, Z. *Polym. Degrad. Stab.* **2013**, *98*, 972–979. DOI: https://doi.org/10.1016/j.polymdegradstab.2013.02.013
26. Zheng, G.; Wu, J.; Wang, W.; Pan, C. *Carbon.* **2004**, *42*, 2839–2847. DOI: https://doi.org/10.1016/j.carbon.2004.06.029
27. Xu, X. B.; et al. *Carbon.* **2005**, *43*, 1479–1487.
28. Bayburdov, T. A.; Shipovskaya, A. B. *Izv. Saratov Univ. New Ser. Chem. Biol. Ecol.* **2018**, *18*, 285–298. DOI: https://doi.org/10.18500/1816-9775-2018-18-3-285-298
29. Smolii, V. A.; Kosarev, A. S.; Yatsenko, E. A. *Glass Ceram.* **2020**, *77*, 94–97. DOI: https://doi.org/10.59957/jctm.v60.i1.2025.510.1007/s10717-020-00247-y
30. Seitnazarova, O.; Kalbaev, A.; Mamataliev, N.; Abdikamalova, A.; Najimova, N. *J. Chem. Technol. Metall.* **2025**, *60*. DOI: https://doi.org/10.59957/jctm.v60.i1.2025.5
31. Mamataliev, N.; Abdikamalova, A.; Eshmetov, I.; Kalbaev, A. *J. Chem. Technol. Metall.* **2023**, *58*. DOI: https://doi.org/10.59957/jctm.v58i6.140
32. Erdogan, F. Freundlich, Langmuir, Temkin, DR and Harkins-Jura. *Int. J. Chem. Reactor Eng.* **2019**, *17*, 20180134. DOI: https://doi.org/10.1515/ijcre-2018-0134
33. Yu, A.; Liu, Y.; Li, X.; Yang, Y.; Zhou, Z.; Liu, H. *Water.* **2021**, *13*, 608. DOI: https://doi.org/10.3390/w13050608